WAVE PROPAGATION THROUGH A VISCOUS FLUID CONTAINED IN A TETHERED, INITIALLY STRESSED, ORTHOTROPIC ELASTIC TUBE

H. B. ATABEK

From the Department of Space Science and Applied Physics, The Catholic University of America, Washington, D. C. 20017

ABSTRACT To give a realistic representation of the pulse propagation in arteries a theoretical analysis of the wave propagation through a viscous incompressible fluid contained in an initially stressed elastic tube is considered. The tube is assumed to be orthotropic and its longitudinal motion is constrained by a uniformly distributed additional mass, a dashpot and a spring. The fluid is assumed to be Newtonian. The analysis is restricted to propagation of small amplitude harmonic waves whose wavelength is large compared to the radius of the vessel. Elimination of arbitrary constants from the general solutions of the equations of motion of the fluid and the wall gives a frequency equation to determine the velocity of propagation. Two roots of this equation give the velocity of propagation of two distinct outgoing waves. One of the waves propagates slower than the other. The propagation properties of s lower waves are very slightly affected by the degree of anisotropy of the wall. The velocity of propagation of faster waves decreases as the ratio of the longitudinal modulus of elasticity to the circumferential modulus decreases; transmission of these waves is very little affected. The influence of the tethering on the propagation velocity of slower waves is negligibly small; transmission of these waves is seriously affected. In tethered tubes faster waves are completely attenuated.

INTRODUCTION

Study of wave propagation through a viscous incompressible fluid contained in an elastic tube is an important problem for those who are interested in the flow of blood in arteries. One can find early history of this problem together with the pertinent references in the review article of Lambossy (1) and in the book by McDonald (2).

Most consistent treatment of the problem was given by Womersley (3). Later, this analysis was extended by Atabek and Lew (4), to cover the effects of circumferential and longitudinal initial stresses. To represent the pulse propagation in arteries properly, these theories still have to be modified to include influences of tethering, anisotropy, and taper of the arterial wall. The effect of tethering was partially considered by Womersley. His model of tethering consists of an additional mass and a spring attached to the arterial wall. However, as was shown by Patel

et al. (5), this model is inadequate to represent longitudinal constraint imposed on the arterial wall by surrounding tissues. Recently Mirsky (6) gave a theory of wave propagation in a viscous fluid contained in an orthotropic elastic tube. His analysis is more general than that of Womersley. It does not require that the thickness over the radius ratio be small. However, his model of longitudinal tethering is the same as Womersley's.

In the present paper, bringing in anisotropic behavior of the arterial wall together with the appropriate tethering, we attempt to extend the theory given by Atabek and Lew to construct a more realistic model of the wave propagation through arteries. Analysis is based on the membrane theory of shells. The membrane theory requires fewer material constants to be known. Experimentally these constants can be determined much more easily than those material constants involved in the thick tube theory. For the thickness over the radius ratio used in numerical calculations by Mirsky, the largest difference between his results and the results of the present theory is less than 3%.

GOVERNING EQUATIONS AND BOUNDARY CONDITIONS

The equations governing the flow phenomenon which is described above are very similar to those given in (4). In the following we will give the governing equations as they are given in this reference and indicate the assumptions which these equations are based on. The flow phenomenon which we are considering, is caused by the interaction of the fluid with the tube. Mathematical statement of the problem includes equations which govern the motion of the fluid, the motion of the tube wall, and also relations (boundary conditions) which connect these two motions with each other.

Hydrodynamics Equations

We assume that fluid is incompressible and Newtonian. We will use cylindrical coordinates r, θ, z, and choose the z-axis along the axis of the tube. We will consider only developed flow. Therefore, the choice of the origin is immaterial.

Fluid flow is governed by Navier-Stokes equations and the equation of continuity. We will assume: flow is axially symmetric, body forces are absent, and magnitudes of the velocity components and their derivatives are so small that their products can be neglected. Under these assumptions governing equations reduce to the following form:

$$\frac{\partial u}{\partial t} = -\frac{1}{\rho}\frac{\partial p}{\partial r} + \nu\left(\frac{\partial^2 u}{\partial r^2} + \frac{1}{r}\frac{\partial u}{\partial r} + \frac{\partial^2 u}{\partial z^2} - \frac{u}{r^2}\right), \tag{1}$$

$$\frac{\partial w}{\partial t} = -\frac{1}{\rho}\frac{\partial p}{\partial z} + \nu\left(\frac{\partial^2 w}{\partial r^2} + \frac{1}{r}\frac{\partial w}{\partial r} + \frac{\partial^2 w}{\partial z^2}\right), \tag{2}$$

$$\frac{1}{r}\frac{\partial}{\partial r}(ru) + \frac{\partial w}{\partial z} = 0. \tag{3}$$

Here t denotes time; u and w denote the components of the fluid velocity along r and z directions, respectively; p is the pressure, ρ is the density, and ν is the kinematic viscosity of the fluid. In the following we will assume that the tube is inflated to a pressure p_0 (measured above the external pressure). Then the pressure p, which enters into equations 1 and 2 will represent the incremental pressure (above p_0) due to wave motion.

Equations of Motion of the Tube

Let ρ_0 denote the density, h the thickness, and a the undisturbed internal radius of the tube. We assume the ratio h/a is small, so that tensile stresses are approximately uniform across the thickness of the tube. Under this assumption, bending moments and shear stresses within the tube are very small and can be neglected. We will also assume that loading and deformation are axially symmetric and the tube is initially inflated with a pressure p_0 and stretched longitudinally.

An element of the wall of the tube will be in equilibrium under the internal and external forces acting on it. Internal forces, under the assumption introduced above, reduce simply to stresses (forces per unit length) T_t and T_θ acting respectively in longitudinal and circumferential directions. We will denote the initial values of these stresses (stresses created by initial inflation and longitudinal stretching) by T_{θ_0} and T_{t_0}. For given values of p_0 and a, we have equation 4

$$T_{\theta_0} = p_0 a. \tag{4}$$

T_{t_0} has to be given independently. Let us note here that a is the radius of the initially inflated tube.

External forces acting on the tube element can be considered in three groups: inertia forces, surface forces due to fluid, and forces of constraint representing the reaction of the surrounding tissue to the motion of arterial wall. Calculation of the first two kinds of external forces were considered in detail previously in (4). Let $\xi = \xi(z, t)$ and $\eta = \eta(z, t)$ be the longitudinal and radial displacements of the wall due to wave motion. Then

$$-\rho_0 h \frac{\partial^2 \xi}{\partial t^2} \quad \text{and} \quad -\rho_0 h \frac{\partial^2 \eta}{\partial t^2} \tag{5}$$

represent the longitudinal and radial components of the inertia forces per unit area.

The forces acting on the inner surface of the tube are due to pressure and friction of the fluid. The longitudinal and radial components of these forces (per unit area) are respectively

$$-\mu \left[\frac{\partial w}{\partial r} + \frac{\partial u}{\partial z}\right]_{r=a} \quad \text{and} \quad \left[p - 2\mu \frac{\partial u}{\partial r}\right]_{r=a}. \tag{6}$$

Here $[\ ]_{r=a}$ indicates that the value of the quantity in the bracket is calculated at $r = a$; μ denotes viscosity of the fluid.

Tethering, the affect of surrounding tissue on the motion of the arterial wall, can be considered as the interaction of two viscoelastic solid media. However this approach makes the problem rather complicated. Let us assume that the response of the surrounding medium can be considered in longitudinal and radial directions independently from each other. Patel et al. (5) showed that within the physiologic range of frequencies, longitudinal tethering of arteries of dogs can be simulated by a mechanical model consisting of a spring, dashpot, and a lumped additional mass. Such a model is represented diagrammatically in Fig. 1. In the following we will adopt this model to represent longitudinal tethering. Furthermore, since there are no comparable studies of radial tethering, we will assume that a similar mechanical model is also capable of simulating the effect of the surrounding tissues on radial motion of the arterial wall.

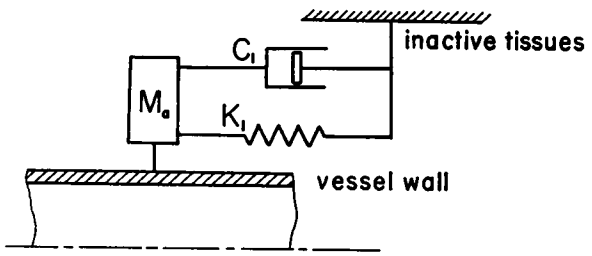

FIGURE 1 The effect of the surrounding tissue on the longitudinal motion of the vessel wall can be simulated by a mechanical model consisting of an additional mass, a dashpot, and a spring.

Let K_l, C_l, and M_a represent respectively (per unit area) the spring coefficient, frictional coefficient of dashpot, and additional mass of the mechanical model of the longitudinal tethering. We will assume that the additional mass of the radial tethering is equal to M_a also. We will denote by K_r and C_r, spring and dashpot coefficients in radial directions. Then the tethering forces (per unit area) acting in longitudinal and radial directions are respectively,

$$-\left(M_a \frac{\partial^2 \xi}{\partial t^2} + C_l \frac{\partial \xi}{\partial t} + K_l \xi\right) \quad \text{and} \quad -\left(M_a \frac{\partial^2 \eta}{\partial t^2} + C_r \frac{\partial \eta}{\partial t} + K_r \eta\right). \tag{7}$$

In equation 5 the factor $\rho_0 h$ represents the mass of the arterial wall per unit area. Taking

$$M_0 = \rho_0 h + M_a \tag{8}$$

we can write the equations for motion of the tube (which express the equilibrium of an element of the wall of the tube under elastic and external forces) as:

$$M_0 \frac{\partial^2 \xi}{\partial t^2} + C_t \frac{\partial \xi}{\partial t} + K_t \xi = -\mu \left[\frac{\partial w}{\partial r} + \frac{\partial u}{\partial z} \right]_{r=a} + \frac{\partial \eta}{\partial z} \frac{T_{t_0} - T_{\theta_0}}{a} + \frac{\partial T_t}{\partial z}, \quad (9)$$

$$M_0 \frac{\partial^2 \eta}{\partial t^2} + C_r \frac{\partial \eta}{\partial t} + K_r \eta = \left[p - 2\mu \frac{\partial u}{\partial r} \right]_{r=a} + \frac{\eta}{a^2} T_{\theta_0} - \frac{T_\theta - T_{\theta_0}}{a} + T_{t_0} \frac{\partial^2 \eta}{\partial z^2}. \quad (10)$$

Equation 9 represents the equilibrium of the longitudinal components of the forces, while equation 10 represents equilibrium of the radial components.

Elasticity Relations

Stress components T_t and T_θ are related to displacement components ξ and η with the constitutive relations. As we have indicated previously, we will measure displacement components from initially stressed state. We assume that displacements corresponding to wave motion are small and they are related to the corresponding excess stresses (stresses measured above initial stresses) linearly.

A body which has three orthogonal planes of elastic symmetry at each point is called orthogonally anisotropic, or shortly, orthotropic. Experiments by Tickner and Sacks (7) and Patel[1] indicate that arteries are orthotropic.

For the axially symmetric deformations of an orthotropic membrane shell, elasticity relations are given by the following formulas (reference 8).

$$T_\theta - T_{\theta_0} = B_{11} \frac{\eta}{a} + B_{12} \frac{\partial \xi}{\partial z}, \quad (11)$$

$$T_t - T_{t_0} = B_{21} \frac{\eta}{a} + B_{22} \frac{\partial \xi}{\partial z}. \quad (12)$$

The coefficients B_{ij} represent stiffnesses along the circumferential and longitudinal directions. For an initially unstressed shell $B_{12} = B_{21}$. On the other hand, for an initially stressed shell, the coefficients B_{ij} depend on initial stresses and in general, $B_{12} \neq B_{21}$ (9). Thus, to describe elastic properties of an initially stressed orthotropic shell we need to know four independent constants.

The coefficients B_{ij} are related to the usual engineering constants.

$$B_{11} = E_\theta h/(1 - \sigma_\theta \sigma_t), \qquad B_{12} = E_\theta h \sigma_t/(1 - \sigma_\theta \sigma_t),$$

$$B_{21} = E_t h \sigma_\theta/(1 - \sigma_\theta \sigma_t), \quad B_{22} = E_t h/(1 - \sigma_\theta \sigma_t).$$

Here E_θ and E_t are Young's moduli in the circumferential and longitudinal directions, respectively; σ_θ and σ_t are the corresponding Poisson's ratios. The constants E_θ, E_t, σ_θ, and σ_t are also functions of the initial stresses. Their values have to be determined, experimentally, in the neighborhood of the initially stressed state.

[1] Patel, D. J. Personal communication.

In calculations which will follow we will use engineering constants. For convenience, let us introduce the following ratios.

$$\gamma_1 = E_t/E_\theta\,, \qquad \gamma_2 = \sigma_t/\sigma_\theta\,. \tag{13}$$

Parameters γ_1 and γ_2 indicate the degree of anisotropy of the vessel wall. For shells which are not initially stressed $\gamma_1 = \gamma_2$.

Boundary Conditions

To complete the description of the problem, we have to supplement the equations given in the previous sections with the boundary conditions. Since fluid particles adhere to the inner surface of the tube, the velocity of the fluid particles on the wall must be equal to the velocity of the wall. When displacements are small, the actual location of the inner surface differs very little from its initial (rest) location, and these boundary conditions can be expressed as

$$u(r, z, t)|_{r=a} = \frac{\partial \eta}{\partial t}\,, \tag{14}$$

$$w(r, z, t)|_{r=a} = \frac{\partial \xi}{\partial t}\,. \tag{15}$$

SOLUTION OF THE PROBLEM

After stating governing equations and boundary conditions we are ready to solve the problem. The equations of motion of the wall are coupled to the equations of motion of fluid through the velocity derivatives and pressure term which they contain. Thus, we are forced to solve hydrodynamics equations first.

Governing equations and boundary conditions are linear. Therefore, solutions for any arbitrary periodic or transient flow phenomenon can be constructed knowing the solution of the problem for a simple harmonic oscillation. We will consider the propagation of forced waves which are harmonic in t and z. We assume that u, w, and p vary in t and z in the following manner.

$$\begin{aligned} u &= \bar{u}(r) \exp\,[i\omega(t - z/c)], \\ w &= \bar{w}(r) \exp\,[i\omega(t - z/c)], \\ p &= \bar{p}(r) \exp\,[i\omega(t - z/c)]. \end{aligned} \tag{16}$$

Here, ω denotes the circular frequency of the forced oscillation and is a real constant; c is the complex propagation velocity.

The general solution of equations 1, 2, and 3 corresponding to the forced harmonic oscillations described by equation 16 was given by Womersley (3). This result is

$$u = \left[- A_1 \frac{\beta_0 a}{\mu \alpha_0^2} J_1 \left(\beta_0 \frac{r}{a} \right) + A_2 \frac{\beta_0}{\alpha_0 J_0(\alpha_0)} J_1 \left((\alpha_0^2 + \beta_0^2)^{1/2} \frac{r}{a} \right) \right] \exp [i\omega(t - z/c)], \quad (17)$$

$$w = \left[- A_1 \frac{\beta_0 a}{\mu \alpha_0^2} J_0 \left(\beta_0 \frac{r}{a} \right) + A_2 \frac{(\alpha_0^2 + \beta_0^2)^{1/2}}{\alpha_0 J_0 (\alpha_0)} J_0 \left((\alpha_0^2 + \beta_0^2)^{1/2} \frac{r}{a} \right) \right] \exp [i\omega(t - z/c)], \quad (18)$$

$$p = A_1 J_0 \left(\beta_0 \frac{r}{a} \right) \exp [i\omega(t - z/c)]. \quad (19)$$

Here A_1 and A_2 are integration constants; $J_0(x)$ and $J_1(x)$ denote the first kind zeroth and first order Bessel functions; α_0 and β_0 are dimensionless parameters and are given by the following relations.

$$\alpha_0^2 = i^3 \frac{a^2 \omega}{\nu} \equiv i^3 \alpha^2, \quad (20)$$

$$\beta_0 = \frac{ia\omega}{c} \equiv i\beta. \quad (21)$$

To determine the integration constants A_1 and A_2 we have to use the boundary conditions (equations 14 and 15). The right-hand side of these conditions involves ξ and η. Since the equations of motion of the wall are linear, the solutions for η and ξ, corresponding to the forced harmonic oscillation given by equation 16, must have the following forms

$$\eta = A_3 \exp [i\omega(t - z/c)], \quad (22)$$

$$\xi = A_4 \exp [i\omega(t - z/c)]. \quad (23)$$

Here A_3 and A_4 are constants to be determined.

Substituting expressions 17, 18, 22, and 23 into the boundary conditions 14 and 15, we obtain the following two algebraic equations for the unknown constants A_1, A_2, A_3, and A_4.

$$- A_1 \frac{\beta_0 a}{\mu \alpha_0^2} J_1(\beta_0) + A_2 \frac{\beta_0}{\alpha_0} \frac{J_1((\alpha_0^2 + \beta_0^2)^{1/2})}{J_0(\alpha_0)} - i\omega A_3 = 0, \quad (24)$$

$$- A_1 \frac{\beta_0 a}{\mu \alpha_0^2} J_0(\beta_0) + A_2 \frac{(\alpha_0^2 + \beta_0^2)^{1/2}}{\alpha_0} \frac{J_0((\alpha_0^2 + \beta_0^2)^{1/2})}{J_0(\alpha_0)} - i\omega A_4 = 0. \quad (25)$$

The equations of motion of the wall (equations 9 and 10) give us two more equations which we need to determine the unknown constants. Using the constitutive equations 11, 12 and the relation 13, we eliminate T_t and T_θ, E_t and σ_t from these equations and obtain

$$M_0 \frac{\partial^2 \eta}{\partial t^2} + C_r \frac{\partial \eta}{\partial t} + K_r \eta = \left[p - 2\mu \frac{\partial u}{\partial r}\right]_a + \frac{\eta}{a^2} T_{\theta_0} + T_{t_0} \frac{\partial^2 \eta}{\partial z^2} - \frac{E_\theta h}{1 - \gamma_2 \sigma_\theta^2} \left(\frac{\eta}{a^2} + \frac{\gamma_2 \sigma_\theta}{a} \frac{\partial \xi}{\partial z}\right), \quad (26)$$

$$M_0 \frac{\partial^2 \xi}{\partial t^2} + C_l \frac{\partial \xi}{\partial t} + K_1 \xi = -\mu \left[\frac{\partial w}{\partial r} + \frac{\partial u}{\partial z}\right]_a + \frac{T_{t_0} - T_{\theta_0}}{a} \frac{\partial \eta}{\partial z} + \frac{\gamma_1 E_\theta h}{1 - \gamma_2 \sigma_\theta^2} \left(\frac{\partial^2 \xi}{\partial z^2} + \frac{\sigma_\theta}{a} \frac{\partial \eta}{\partial z}\right). \quad (27)$$

Substituting equations 17–19, 22, and 23 first into equation 25 and then into 27, we obtain the following two algebraic equations for the unknown constants A_1, A_2, A_3, and A_4.

$$A_1 \left[J_0(\beta_0) + \frac{\beta_0^2}{a\alpha_0^2} (J_0(\beta_0) - J_2(\beta_0))\right] - A_2 \frac{\mu\beta_0}{a\alpha_0 J_0(\alpha_0)} \cdot [J_0((\alpha_0^2 + \beta_0^2)^{1/2}) - J_2((\alpha_0^2 + \beta_0^2)^{1/2})] + A_3 \left[\left(T_{t_0}\beta_0^2 + T_{\theta_0} - \frac{E_\theta h}{1 - \gamma_2 \sigma_\theta^2}\right)\frac{1}{a^2} + \omega^2 \left(M_0 - i\frac{C_r}{\omega} - \frac{K_r}{\omega^2}\right)\right] + A_4 \frac{E_\theta h}{1 - \gamma_2 \sigma_\theta^2} \frac{\gamma_2 \sigma_\theta \beta_0}{a^2} = 0, \quad (28)$$

$$-A_1 \frac{2\beta_0}{\alpha_0^2} J_1(\beta_0) + A_2 \frac{\mu(\alpha_0^2 + 2\beta_0^2)}{a\alpha_0 J_0(\alpha_0)} J_1((\alpha_0^2 + \beta_0^2)^{1/2}) - A_3 \frac{\beta_0}{a^2} \left(\frac{\gamma_1 E_\theta h \sigma_\theta}{1 - \gamma_2 \sigma_\theta^2} + T_{t_0} - T_{\theta_0}\right) + A_4 \left[\frac{\gamma_1 E_\theta h}{1 - \gamma_2 \sigma_\theta^2} \frac{\beta_0^2}{a^2} + \omega^2 \left(M_0 - i\frac{C_l}{\omega} - \frac{K_l}{\omega^2}\right)\right] = 0. \quad (29)$$

Equations 24, 25, 28, and 29 constitute a system of homogeneous algebraic equations for the constants A_1, A_2, A_3, A_4 and will have nontrivial solutions if the determinant of the coefficient is zero. Equating this determinant to zero, we obtain the frequency equation in which the only unknown is the complex velocity of propagation c. As a quick inspection of the coefficient of equations 24, 25, 28, and 29 reveals, the frequency equation is rather complicated. To simplify this equation, as is done previously in [4] we will assume that the wavelengths of the oscillations are very large compared with the radius of the tube.

This assumption is equivalent to $|\beta_0| = |a\omega/c| \ll 1$. For very small values of $|\beta_0|$, we have

$$J_0(\beta_0) \simeq 1, \qquad J_1(\beta_0) \simeq \frac{\beta_0}{2}, \qquad J_2(\beta_0) \simeq \frac{1}{8}\beta_0^2, \qquad \alpha_0^2 + \beta_0^2 \simeq \alpha_0^2. \quad (30)$$

When we substitute these relations into equations 24, 25, 28, and 29 we obtain the following set of algebraic equations for A_1, A_2, A_3, and A_4

$$-\frac{\beta_0^2 a}{2\mu\alpha_0^2}A_1 + \frac{1}{2}\beta_0 F_{10}A_2 - i\omega A_3 = 0, \tag{31}$$

$$-\frac{\beta_0 a}{2\mu\alpha_0^2}A_1 + A_2 - i\omega A_4 = 0, \tag{32}$$

$$A_1 - \frac{\mu\beta_0}{a}(2 - F_{10})A_2 + \left[T_{t_0}\frac{\beta_0^2}{a^2} + \frac{T_{\theta_0}}{a^2} - \frac{E_\theta h}{1 - \gamma_2\sigma_\theta^2}\frac{1}{a^2} + \omega^2\left(M_0 - i\frac{C_r}{\omega} - \frac{K_r}{\omega^2}\right)\right]A_3 + \frac{E_\theta h}{1 - \gamma_2\sigma_\theta^2}\frac{\gamma_2\sigma_\theta\beta_0}{a^2}A_4 = 0, \tag{33}$$

$$-\frac{\beta_0^3}{\alpha_0^2}A_1 + \frac{\mu\alpha_0^2}{2a}F_{10}A_2 - \left(\frac{\gamma_1 E_\theta h}{1 - \gamma_2\sigma_\theta^2}\sigma_\theta + T_{t_0} - T_{\theta_0}\right)\frac{\beta_0}{a^2}A_3 + \left[\frac{\gamma_1 E_\theta h}{1 - \gamma_2\sigma_\theta^2}\frac{\beta_0^2}{a^2} + \omega^2\left(M_0 - i\frac{C_l}{\omega} - \frac{K_l}{\omega^2}\right)\right]A_4 = 0. \tag{34}$$

Here

$$F_{10} = 2J_1(\alpha_0)/\alpha_0 J_0(\alpha_0). \tag{35}$$

In equation 33 the coefficient of A_3 can be simplified. Indeed as was shown in (4), within the physiological range of the appropriate parameters, the term $T_{t_0}\beta_0^2/a^2$ can be neglected in comparison with the two terms which follow it. The order of magnitude of the term $\omega^2[M_0 - (iC_r/\omega) - (K_r/\omega^2)]$ depends, besides ω, on the values of the parameters M_0, C_r, and K_r. As we mentioned previously there is no available information with regard to the parameters C_r and K_r. Under this condition we may intuitively assume that $C_r \simeq C_l$ and $K_r \simeq K_l$. When this assumption is accepted, it can be shown that the term $\omega^2[M_0 - (iC_r/\omega) - (K_r/\omega^2)]$ is indeed much smaller than the remaining terms of the coefficient of A_3. In the following we will adopt this assumption. With this simplification, the effect of radial tethering completely drops out of the equation system.

Equating the determinant of the coefficients of the equations 31–34 to zero we obtain the frequency equation.

$$\begin{vmatrix} -\frac{\beta_0^2 a}{2\mu\alpha_0^2} & \frac{\beta_0 F_{10}}{2} & -i\omega & 0 \\ -\frac{\beta_0 a}{2\mu\alpha_0^2} & 1 & 0 & -i\omega \\ 1 & -\frac{\mu\beta_0}{a}(2 - F_{10}) & \left(T_{\theta_0} - \frac{E_\theta h}{1 - \gamma_2\sigma_\theta^2}\right)\frac{1}{a^2} & \frac{E_\theta h}{1 - \gamma_2\sigma_\theta^2}\frac{\gamma_2\sigma_\theta\beta_0}{a^2} \\ -\frac{\beta_0^3}{\alpha_0^2} & \frac{\mu\alpha_0^2}{2a}F_{10} & \left(-\frac{\gamma_1 E_\theta h}{1 - \gamma_2\sigma_\theta^2}\sigma_\theta + T_{t_0} - T_{\theta_0}\right)\frac{\beta_0}{a^2} & \frac{\gamma_1 E_\theta h}{1 - \gamma_2\sigma_\theta^2}\frac{\beta_0^2}{a^2} + \omega^2\left(M_0 - \frac{iC_l}{\omega} - \frac{K_l}{\omega^2}\right) \end{vmatrix} = 0. \tag{36}$$

This equation is very similar to the corresponding frequency equation given in (4). Therefore, without going through intermediate steps of algebra here, we will give the final form of the frequency equation.

$$\frac{4(1-F_{10})}{(1-\gamma_2\sigma_\theta^2)^2}[\gamma_1(1-\tau_\theta)-\gamma_2\sigma_\theta(\gamma_1\sigma_\theta+\tau_t-\tau_\theta)]\frac{c_0^4}{c^4}$$
$$+\frac{2}{1-\gamma_2\sigma_\theta^2}\Big[-k(1-F_{10})(1-\tau_\theta)+F_{10}\Big((\gamma_1+\gamma_2)\sigma_\theta$$
$$+\tau_t-\frac{1}{2}\tau_\theta-\frac{1}{2}\Big)-2\gamma_1\Big]\frac{c_0^2}{c^2}+F_{10}+2k=0. \quad (37)$$

The dimensionless parameters

$$\tau_\theta = T_{\theta_0}/[E_\theta h/(1-\gamma_2\sigma_\theta)], \qquad \tau_t = T_{t_0}/[E_\theta h/(1-\gamma_2\sigma_\theta^2)]$$

represent the effect of circumferential and longitudinal initial stresses. c_0 denotes Moens-Korteweg wave velocity and is given by the following formula.

$$c_0 = (E_\theta h/2a\rho)^{1/2}.$$

The complex number

$$k = M - i\frac{C}{\alpha^2} - \frac{K}{\alpha^4} \quad (38)$$

represents the effect of total tethering. M, C, and K are dimensionless parameters.

$$M = \frac{M_0}{a\rho}, \qquad C = \frac{C_l a}{\mu}, \qquad K = \frac{K_l a^3\rho}{\mu^2}.$$

In the given order these parameters represent the contributions of the inertial, viscous, and elastic constraints to the total tethering.

For $\gamma_1 = \gamma_2 = 1$, $C = K = 0$, equation 37 reduces to the frequency equation given in reference 4. The roots of equation 37 are complex numbers. Let us represent them as

$$c_0/c = X - iY.$$

Since

$$\exp[i\omega(t - z/c)] = \exp[i\omega(t - zX/c_0)]\exp[-2\pi(z/\lambda)(Y/X)],$$

where λ is the wavelength of the oscillation, we see that c_0/X gives us the velocity of propagation of wave and $\exp(-2\pi Y/X)$ represents transmission per wavelength.

Equation 37 being a quadratic equation in $(c_0/c)^2$, two of its four roots

differ from the other two only in sign. Two of these solutions (for which $X > 0$) represent outgoing waves, i.e. the waves which are propagating in positive z directions. The other two roots ($X < 0$) represent incoming waves. We will consider only outgoing waves. As was shown by Atabek and Lew, the velocity of propagation of one of the outgoing waves is smaller. We call this a first-kind wave and denote its propagation velocity by c_1. We will denote the velocity of propagation of the second-kind wave by c_2.

Propagation properties of waves depend on the influence of the parameters τ_θ, τ_t, σ_θ, γ_1, γ_2, M, C, and K. The influence of the parameters τ_θ and τ_t on propagation properties was previously analyzed by Atabek and Lew (4). The effect of the parameter σ_θ and the combined effect of the parameters M and K were investigated by Womersley (3). There is no experimental information available as yet for the parameter γ_2. For the numerical calculations we will assume $\gamma_2 = \gamma_1$ and denote their common value by γ.

In the following, besides studying the influence of the parameters γ and C on the propagation properties, we will also reconsider the effects of the parameters M and K individually. We will take the following values of the parameters as the basis:

$$\tau_\theta = 0, \quad \tau_t = 0, \quad \sigma_\theta = 0.5, \quad \gamma = 1, \quad M = 0.15, \quad K = 0, \quad C = 0.$$

These values of the parameters represent a free, isotropic tube.[2]

To study the effect of a particular factor we will vary the corresponding parameter, within a physiologically meaningful interval, while keeping all the others fixed in their base values. In choosing the interval of variation for the parameters, we are guided by the following values of these parameters which approximately represent descending aorta of dogs:

$$\tau_\theta = 0.1, \ \tau_t = 0.09, \ \sigma_\theta = 0.51, \ \gamma = 0.63, \ M = 0.70, \ C = 550, \ K = 1.6 \times 10^6.$$

These values of the dimensionless parameters are calculated from the experimental results obtained by Patel et al. (5)[1].

Before we start to consider the effects of different factors, we will pause here to correct an error in the paper of Atabek and Lew (4). This correction is important for the proper understanding of the wave propagation phenomenon in initially stressed tubes. Atabek and Lew in carrying out numerical calculations, made a sign error in one of the terms of the frequency equation. As a result of this mistake, some of the figures representing the effects of τ_t on propagation properties, appear to be wrong. Table I is given both to correct this mistake and to summarize previously obtained results.

[2] Strictly speaking when $\gamma = 1$, the value of Poisson's ratio must be always less than $\frac{1}{2}$. For an isotropic tube $\sigma_\theta = \frac{1}{2}$ implies incompressibility. The elasticity relations which are used in this theory are not valid for incompressible materials.

TABLE I

	c_1/c_0	Transmission of first-kind wave	c_2/c_0	Transmission of second-kind wave
As τ_θ increases	decreases	decreases	increases	increases
As τ_t increases	decreases	increases	decreases	decreases
As σ_θ increases	increases	increases	increases	decreases

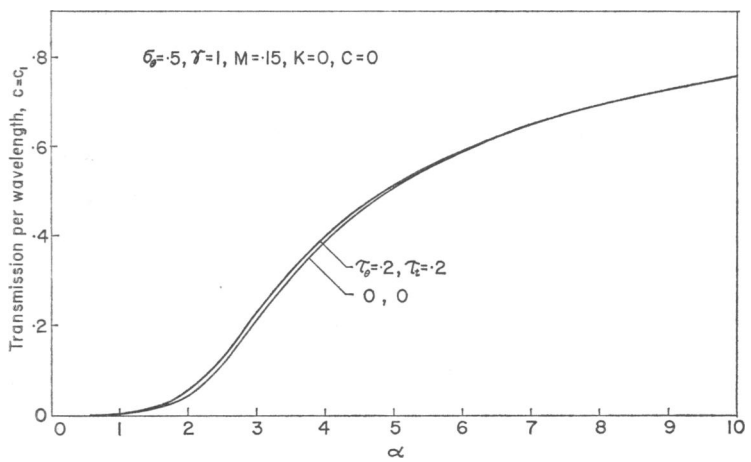

FIGURE 2 The influences of the circumferential and longitudinal initial stresses on the transmission of the first-kind waves oppose each other.

The most important fact which comes out of this correction is that the circumferential and longitudinal initial stresses generate opposite effects on the transmission of the first-kind waves. This may help us to understand the role of the longitudinal initial stresses in arteries. The velocity of propagation c_1/c_0 through a vessel may be lowered increasing τ_θ (increasing p_0). However, as τ_θ increases transmission gets worse. Increasing τ_t one may counteract this, which also helps to decrease c_1/c_0 further. Fig. 2 represents the effect of combined initial stresses on transmission of the first-kind waves.

Figs. 3 and 4 represent variation of velocity of propagation and transmission of the first-kind wave vs. α for different values of the anisotropy parameter γ. Except for the small values of α, influence of anisotropy on propagation properties of these waves is negligible. On the other hand, as is shown in Fig. 5, velocity of propagation of the second-kind wave is seriously affected by anisotropy. For small values of α, transmission of these waves increases as γ decreases (see Fig. 6). These results agree closely with those of Mirsky (6).

In Figs. 7–10 we show the effect of the total mass of the vessel and the surrounding tissues on the propagation properties of the first and second-kind waves. As M increases both c_1/c_0 and c_2/c_0 decrease and corresponding transmissions increase.

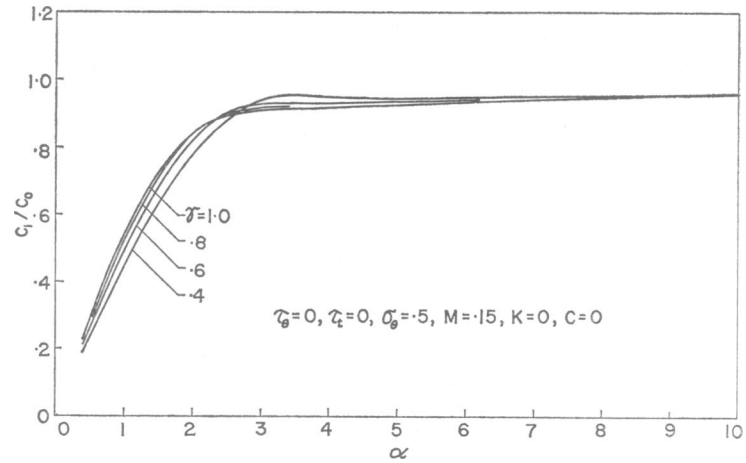

FIGURE 3 The value of the parameter $\gamma(= E_t/E_\theta = \sigma_t/\sigma_\theta)$ is an indication of the degree of anisotropy of the vessel wall. For large values of α, c_1/c_0 is unaffected by anisotropy.

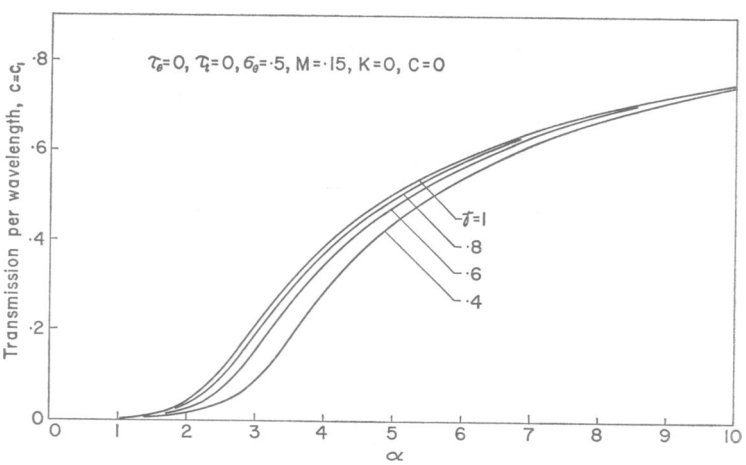

FIGURE 4 For large values of α, the transmission of the first-kind waves is also unaffected by the anisotropy of the tube wall.

Similar increments in M produce larger influences on the second waves. This in part can be explained remembering that the second-kind wave, essentially, propagates through the vessel wall (4).

The effects of the parameters C and K are very similar. Figs. 11 and 12 represent the velocity of propagation of the first kind waves vs. α as functions of the parameters C and K. As the parameter C (or K) increases, the value of c_1/c_0 increases. On the other hand, as can be seen from Figs. 13 and 14, for a given value of α, as the parameters C and K increase, transmissions of the first-kind waves decrease. The influence of the parameters C and K diminishes as α increases. This and the

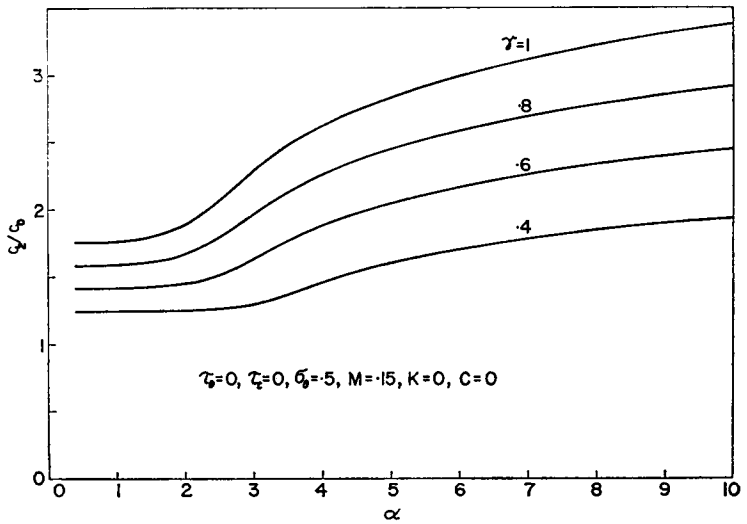

FIGURE 5 As the anisotropy of the vessel wall increases, the velocity of propagation of the second-kind waves decreases significantly.

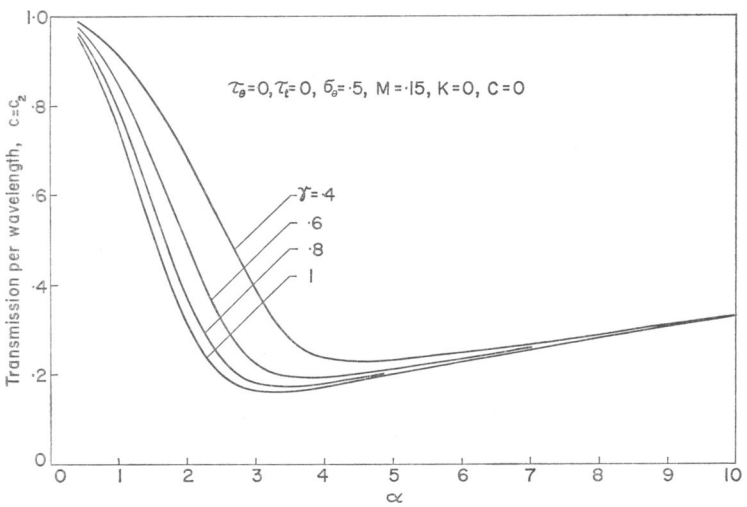

FIGURE 6 For large values of α, the transmission of the second-kind waves is not affected by the anisotropy of the wall.

somewhat strange behavior of all these curves can be explained through equation 38.

Small increments of parameters C and K produce large effects on the properties of the second-kind waves. In Figs. 15 and 16 we give the variation of transmission of these waves vs. α as functions of the parameters C and K. For large values of C

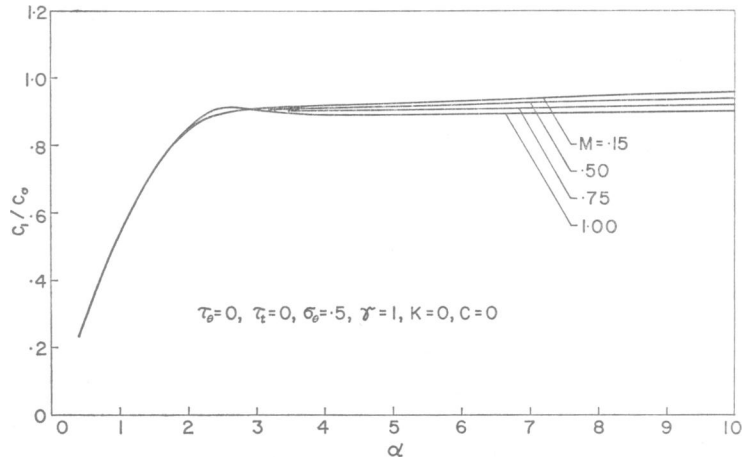

FIGURE 7 The variation of c_1/c_0 as a function α is shown for the different values of M. The parameter M represents the total inertial constraint on the wall of the tube.

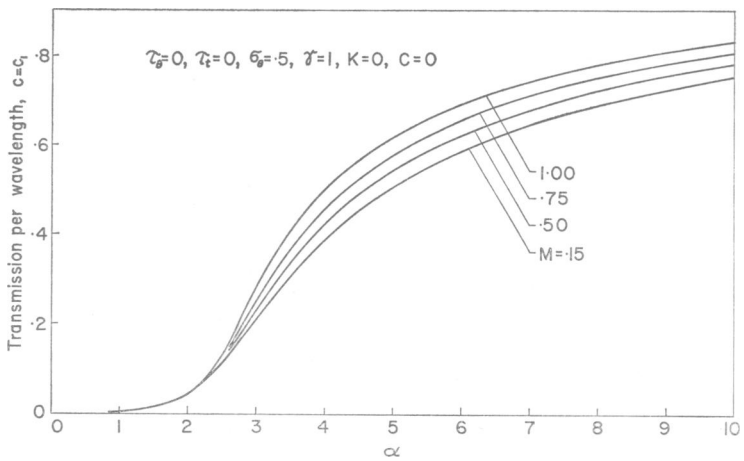

FIGURE 8 The variation of the transmission per wavelength of the first-kind waves vs. α as a function of the parameter M.

and K second-kind waves are completely attenuated within the usable range of α.

The effect of the parameter C is to reduce c_2/c_0. On the other hand, as K increases, c_2/c_0 increases tremendously. Because of their very poor transmission properties second-kind waves lose their importance.

In Figs. 17 and 18 the propagation properties of the first-kind waves through totally tethered and free tubes are plotted as functions of α. From these figures we see that although the influence of tethering on the propagation velocity is negligibly small, transmission through a tethered tube is substantially lower than that through the free tube.

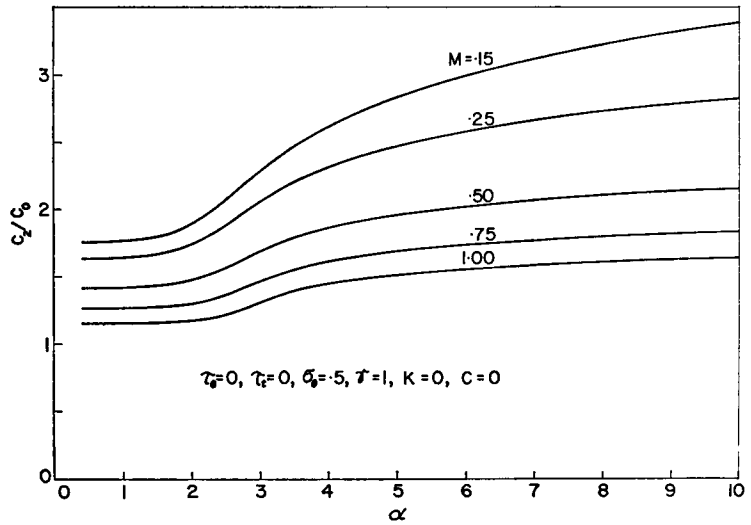

FIGURE 9. The effect of inertial constraint is to decrease the velocity of propagation of the second-kind waves.

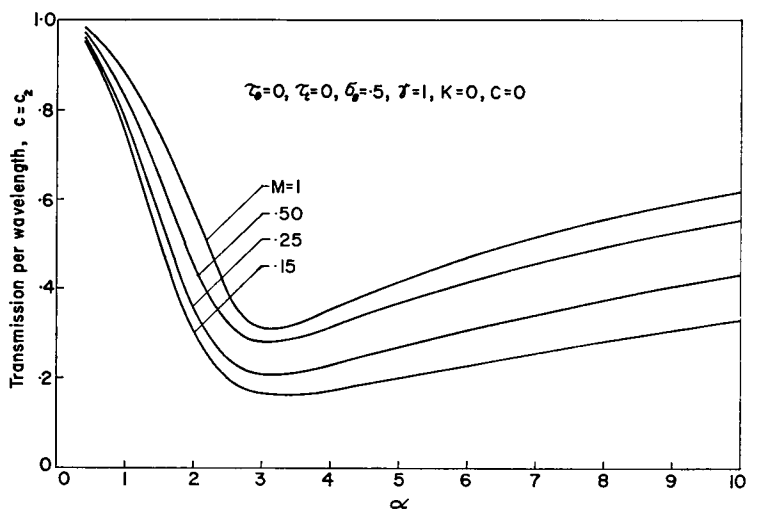

FIGURE 10 As the parameter M increases, the transmission of the second-kind waves improves.

After determining c we can go back to the system of equations 31–34 and determine the integration constants A_1, A_2, A_3, and A_4. We will express the constants A_2, A_3, and A_4 in terms of the constant A_1. Constant A_1 representing the magnitude of the incremental pressure is a directly measurable quantity. Solving the system

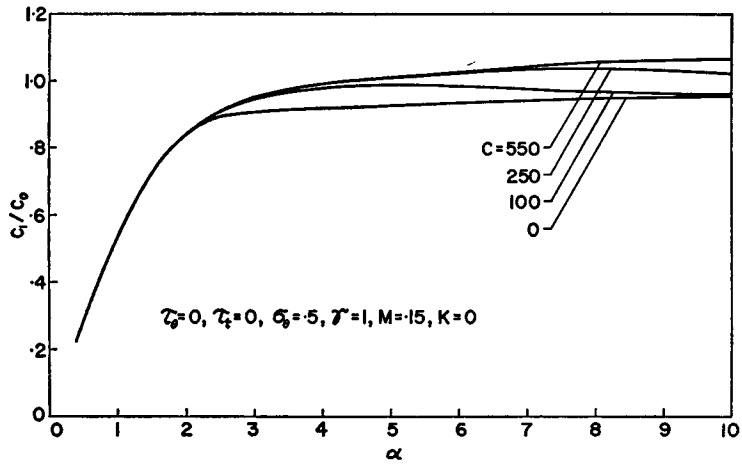

FIGURE 11 The influence of the viscous constraint is to increase the ratio c_1/c_0. For large values of α all the curves converge toward the curve $C = 0$.

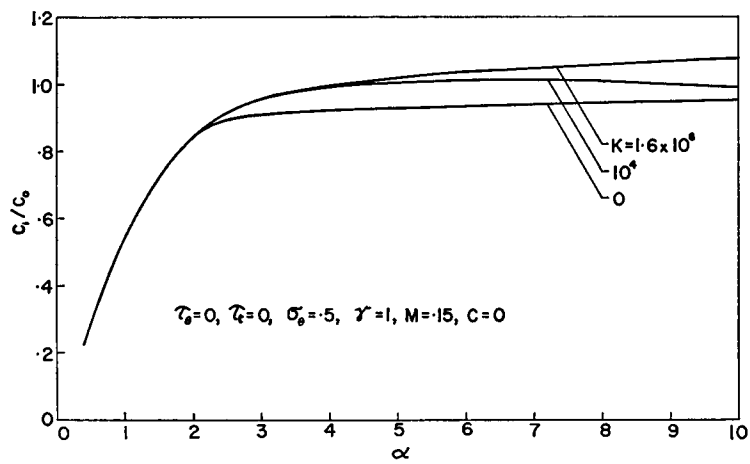

FIGURE 12 The parameter K represents the elastic constraint imposed on the vessel wall. c_1/c_0 increases with K. The influence of K dies out slowly as α increases.

we obtain

$$A_2 = A_1 \frac{m}{\rho c}, \tag{39}$$

$$A_3 = A_1 \frac{a}{2\rho c^2}(1 + F_{10} m), \tag{40}$$

$$A_4 = -A_1 \frac{i}{\omega \rho c}(1 + m), \tag{41}$$

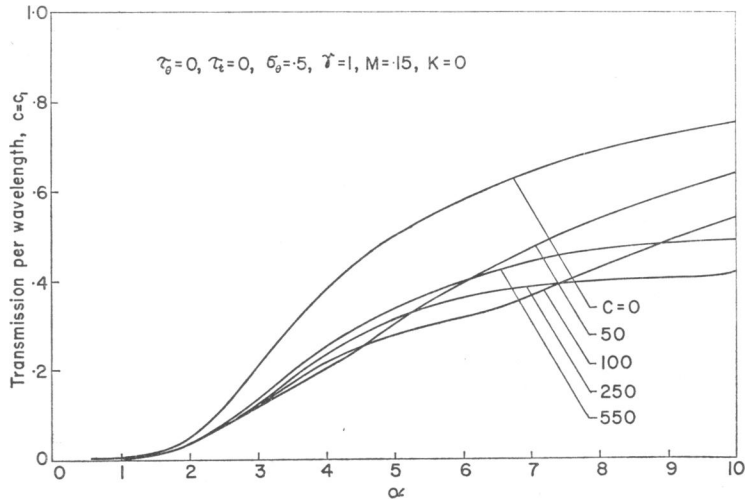

FIGURE 13 The influence of the viscous constraint is to decrease the transmission of the first-kind waves. For large values of α, viscous constraint ceases to be effective and all curves converge toward the curve $C = 0$.

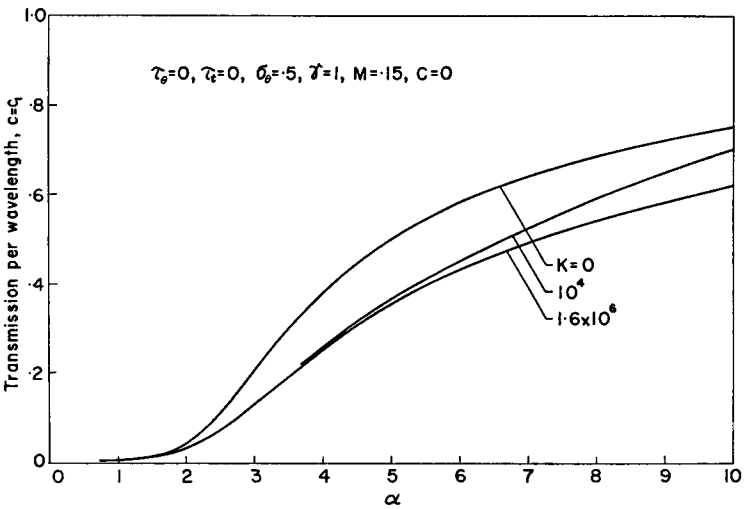

FIGURE 14 The influence of the elastic constraint on transmission of the first-kind waves is similar to that of viscous constraint.

where

$$m = \frac{[2\gamma_2 \sigma_\theta - (1 - \tau_\theta)]\, c_0^2/c^2 + 1 - \gamma_2 \sigma_\theta^2}{[(1 - \tau_\theta)F_{10} - 2\gamma_2 \sigma_\theta]\, c_0^2/c^2}. \tag{42}$$

Now, we are ready to write down the final form of the expressions for the velocity and displacement components. Carrying equations 39–41 together with equation

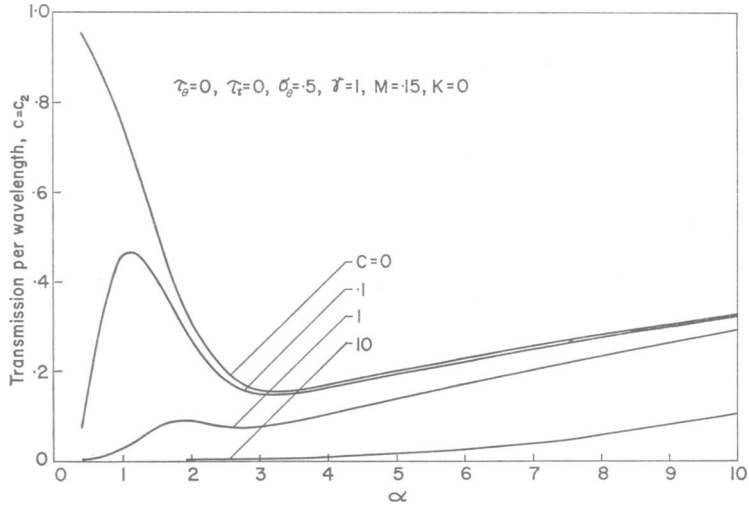

FIGURE 15 The viscous constraint is very effective in controlling the transmission of the second-kind waves. For the physiologically normal values of the parameter C, these waves are almost completely suppressed within the usable range of α.

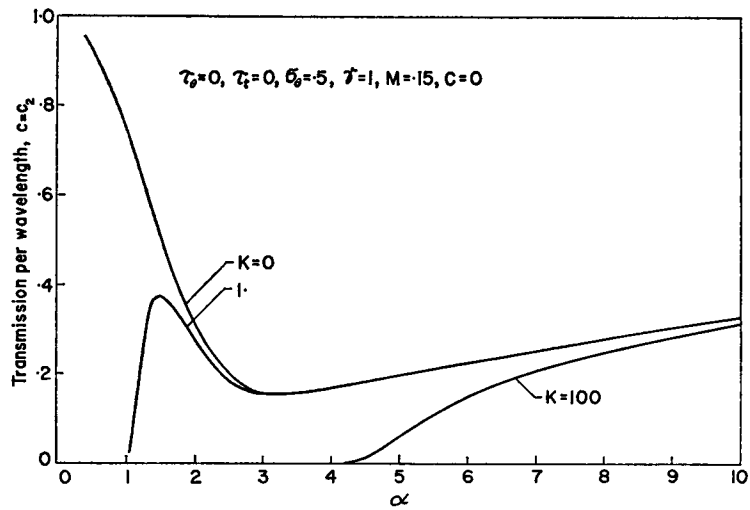

FIGURE 16 The elastic constraint is much more effective than the viscous constraint in suppressing the transmission of the second-kind waves.

30 into equations 17–19, 22, and 23, we obtain

$$u = A_1 \frac{\beta}{c\rho} i \left[\frac{r}{2a} + m \frac{J_1\left(\alpha_0 \frac{r}{a}\right)}{\alpha_0 J_0(\alpha_0)} \right] \exp\left[i\omega(t - z/c)\right], \tag{43}$$

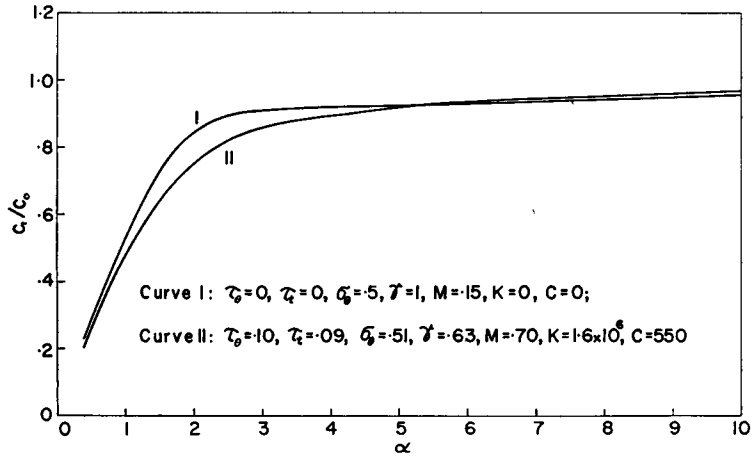

FIGURE 17 The influence of the total tethering on c_1/c_0 is almost negligible.

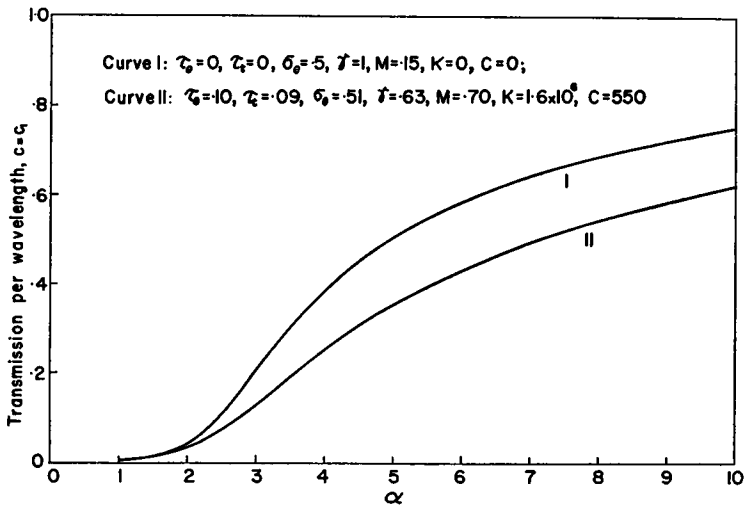

FIGURE 18 The transmission of the first-kind waves is seriously affected by the total tethering.

$$w = A_1 \frac{1}{c\rho}\left[1 + m\frac{J_0\left(\alpha_0 \frac{r}{a}\right)}{J_0(\alpha_0)}\right] \exp\,(i\omega(t - z/c)], \tag{44}$$

$$p = A_1 \exp\,[i\omega(t - z/c)], \tag{45}$$

$$\eta = A_1 \frac{a}{2\rho c^2}\,(1 + F_{10}\,m)\,\exp\,[i\omega(t - z/c)], \tag{46}$$

$$\xi = -A_1 \frac{i}{\omega\rho c}\,(1 + m)\,\exp\,[i\omega(t - z/c)]. \tag{47}$$

Comparing equations 45 and 46 we see that the radial displacement of the vessel is directly related to the incremental pressure. Indeed substituting equation 45 into 46 and rearranging the terms we get the following dimensionless combination between η and p.

$$\left(\frac{\eta}{a}\right) \Big/ \left(\frac{p}{\rho c_0^2}\right) = \frac{1}{2}\frac{c_0^2}{c^2}(1 + F_{10}\, m). \tag{48}$$

The right-hand side of equation 48 for a given vessel-fluid system depends only on the parameter α. Let us denote the modulus and the argument of this complex number by M and ψ, respectively. In Fig. 19 we give the variation of M and ψ as a function of the parameter α, for both the free and tethered tubes. In the interval $1.5 < \alpha < 12$ the phase angle of the tethered tube, ψ_T, is equal to zero. In this interval the wall displacement of the tethered tube is directly proportional to the incremental pressure. Starting from zero at $\alpha = 12$, ψ_T decreases slowly and after passing through a minimum at $\alpha = 44$, where it is equal to $-2.17°$, it begins to rise toward zero again. This phase lag is caused by the viscous constraint. On the other hand, ψ_F, staying always positive, decreases gradually toward zero. Its value at $\alpha = 50$ is 0.34°.

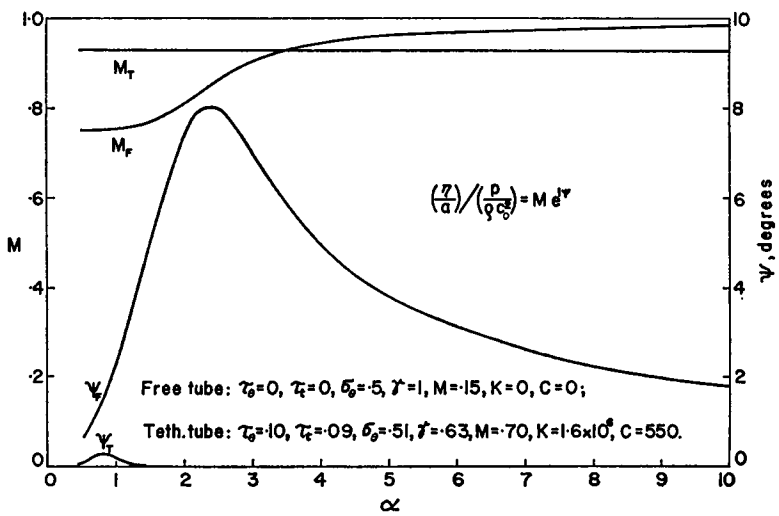

FIGURE 19 In the interval $1.5 < \alpha < 12$, the radial displacement of a tethered tube is proportional to the incremental pressure. For $\alpha > 12$, the phase angle of displacement lags slightly behind that of incremental pressure.

Excessively large longitudinal displacement has been one of the main sources of dissatisfaction with the free tube theory. Now, after bringing in full tethering effect in the longitudinal direction it is interesting to investigate the longitudinal displace-

ment. Combining equations 46 and 47 and rearranging terms we obtain

$$\frac{a\omega}{c_0}\frac{\xi}{\eta} = -2i\frac{c}{c_0}\frac{1+m}{1+mF_{10}}. \tag{49}$$

For a given vessel-fluid system, the right-hand side of this equation depends only on the parameter α. In Fig. 20 we have plotted the modulus of the displacement ratio, $a\omega/c_0|\,\xi/\eta\,|$ vs. α for the free and tethered tubes. For the free tube, for $\alpha > 3$ this ratio is practically constant. On the other hand, for the tethered tube, this ratio after passing through a minimum around $\alpha = 3.7$ increases steadily and con-

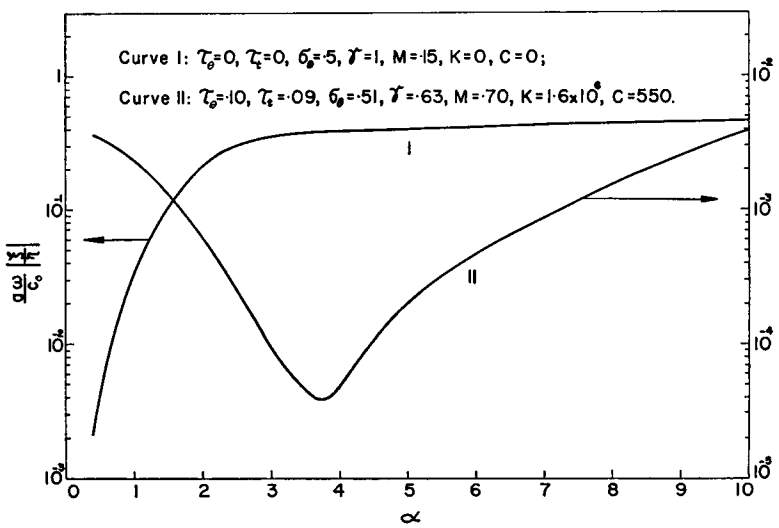

FIGURE 20 The longitudinal displacement of the wall is seriously affected by the total tethering. At $\alpha = 10$, the displacement ratio of the free tube is approximately 100 times larger than that of the tethered tube.

verges toward the free tube value. In view of equation 38, for large values of α, tethering ceases to be effective.

CONCLUDING REMARKS

The theory given above is based on the membrane theory. In the engineering practice the membrane theory is used to calculate those thin shells which are incapable of sustaining compression loads. Thin shell means that $h/a \simeq 0.05$. If one accepts the usual concept of thickness of an artery, clearly this criterion is not satisfied.

Arterial wall is inhomogeneous. The mechanical properties of the layers which compose the wall are all different. And these layers definitely do not carry equal loads. At normal blood pressures, elastic and muscular tissues support wall tension, and the rest of the wall participates weakly (10). If one takes h to be the total

thickness of these active layers, the requirement that h/a be small might be satisfied. In this case the rest of the material of the wall can be considered as additional mass.

In calculations, Young's modulus and thickness always come in the combination of $E_\theta h$. This is also true for experiments. The force, not the stress, can be measured directly. To determine Young's modulus one has to know the thickness. Measurement of the arterial wall thickness in vivo is a very difficult task. Under these circumstances, it is clear that the ordinary definitions of thickness and Young's modulus are artificial. It is more reasonably to use the combination $E_\theta h$ as a characteristic quantity, instead of dealing with Young's modulus and the thickness separately.

To represent wave propagation through arteries, the theory described above is incomplete. The effects of taper, branching, and viscoelastic properties of the arterial wall have not been considered. The theory is also an approximate one. We had to introduce certain simplifying assumptions. The most important one of these is our neglect of the nonlinear terms of the Navier-Stokes equations. The effect of nonlinear terms on pulse propagation was considered by Lambert (11), Streeter et al. (12), Olsen (13), and Barnard et al. (14). These investigators attacked the problem either by neglecting the effect of fluid viscosity (11) or by replacing the viscous terms of the Navier-Stokes equations with a "friction term" which is a function of the longitudinal component of the velocity. The friction term was calculated (or chosen) by "assuming" that the velocity distribution across the vessel lumen was known. All these theories provide description of pulse wave propagation and flow contours that are plausible.

The flow phenomenon in arteries is not simply a problem of pulse propagation. A complete description of the flow should definitely include detailed knowledge of velocity distribution across the lumen as a function of time. This is necessary to answer many recent questions which have arisen in the areas of pathology, diagnosis, and therapy. For example, recent work by Fry (15) has demonstrated that the endothelial surface is sensitive to adjacent hydrodynamic events. It has been shown that endothelial cells have a yield stress of about 350 dynes/cm^2. Exposure to a shearing stress in excess of this for periods of only 1 hr will cause severe endothelial damage. Since these increased shearing stresses were produced artificially, the question remains as to whether stresses such as these ever occur in the normally functioning vascular bed. This information can only be obtained from detailed knowledge of the velocity distribution.

In studying this problem the author's main aim has been to prepare the necessary foundation for calculating the flow of blood in arteries. Indeed, as was done by Womersley (3) and others, one can use equations 43–45 and harmonic analysis to calculate velocity and pressure distribution along the arteries. This method provides results which agree reasonably well with the experiments (see reference 3). However let us note here that experiments conducted so far deal only with the gross behavior of the flow such as measurement of discharge rate and apparent phase velocity.

The critical evaluation of this and the other existing theories requires detailed measurement of velocity distribution together with pressure as a function of time. Presently Ling (16) and his associates, using hot-film anemometer, are conducting such measurements in elastic tubes and simulating models.

This work is supported by the Department of Health, Education, and Welfare, NIH, under the Grants HE 08848-02 and -03.

Received for publication 22 January 1968.

REFERENCES

1. LAMBOSSY, P. 1951. *Helv. Physiol. Pharmacol. Acta.* **9**:145.
2. MCDONALD, D. A. 1960. Blood Flow in Arteries. The Williams and Wilkins Co., Baltimore, Md.
3. WOMERSLEY, J. R. 1957. An Elastic Tube Theory of Pulse Transmission and Oscillatory Flow in Mammalian Arteries. Wright Air Development Center Technical Report TR 56-6114. Wright-Patterson AFB, Ohio.
4. ATABEK, H. B., and H. S. LEW. 1966. *Biophys. J.* **6**:481.
5. PATEL, D. J., D. L. FRY, and J. S. JANICKI. 1966. *Circulation Res.* **19**:1011.
6. MIRSKY, I. 1967. *Biophys. J.* **7**:165.
7. TICKNER, E. G., and A. H. SACKS. 1964. Theoretical and Experimental Study of the Elastic Behavior of the Human Brachial and Other Human and Canine Arteries. Report No. 161. Vidya Co., Palo Alto, Calif.
8. AMBARTSUMYAN, S. A. 1964. Theory of Anisotropic Shells. NASA TT F-118. Washington, D. C.
9. BIOT, M. A. 1965. Mechanics of Incremental Deformations. John Wiley & Sons, Inc., New York.
10. BADER, H. 1963. Handbook of Physiology, Circulation. W. F. Hamilton, editor. American Physiological Society, Washington, D. C. Vol. II, Chap. 26.
11. LAMBERT, J. W. 1958. *J. Franklin Inst.* **266**:83.
12. STREETER, V. L., W. F. KREITZER, and D. F. BOHR. 1964. Pulsatile Blood Flow. E. O. Attinger, editor. McGraw-Hill Book Co., New York. Chap. 8.
13. OLSEN, J. H. 1966. Doctoral thesis. Mass. Inst. Technol., Cambridge, Mass.
14. BARNARD, A. C. L., W. A. HUNT, W. P. TIMLAKE, and E. VARLEY. 1966. *Biophys. J.* **6**:717.
15. FRY, D. L. 1968. *Circulation Res.* **22**:156.
16. LING, S. C. 1967. *Proc. Ann. Conf. Eng. Med. Biol.* **9**:6.6.